Hindawi
Advances in Materials Science and Engineering
Volume 2022, Article ID 8761865, 8 pages
https://doi.org/10.1155/2022/8761865

Research Article

Characterization of the Aluminium Matrix Composite Reinforced with Silicon Nitride ($AA6061/Si_3N_4$) Synthesized by the Stir Casting Route

B. Ashok Kumar,[1] **M. Muthu Krishnan**,[2] **A. Felix Sahayaraj**,[2] **Mohamad Reda A. Refaai**,[3] **G. Yuvaraj**,[4] **D. Madhesh**,[5] **and Haiter Lenin Allasi**[6]

[1]*Department of Mechanical Engineering, Nandha Engineering College, Vaikkaal Medu, Erode 638052, Tamil Nadu, India*
[2]*Department of Mechanical Engineering, Kalaignar Karunanidhi Institute of Technology, Coimbatore 641402, Tamil Nadu, India*
[3]*Prince Sattam bin Abdulaziz University, College of Engineering, Department of Mechanical Engineering, Alkharj 16273, Saudi Arabia*
[4]*Department of Mechanical Engineering, Easwari Engineering College, Chennai 600089, Tamil Nadu, India*
[5]*Department of Mechanical Engineering, Academy of Maritime Education and Training (AMET), Chennai 603112, Tamil Nadu, India*
[6]*Department of Mechanical Engineering, Wollo University, Kombolcha Institute of Technology, Kombolcha, Ethiopia*

Correspondence should be addressed to Haiter Lenin Allasi; drahlenin@kiot.edu.et

Received 25 October 2021; Accepted 4 January 2022; Published 29 January 2022

Academic Editor: P. Ganeshan

The current work is concerned with the synthesis of aluminium (AA6061-T6) matrix composites (AMCs) reinforced with 15 and 20 weight percentages of silicon nitride (Si_3N_4) particulates using the indigenously fabricated electric stir casting furnace with bottom discharge arrangement. The major concern in the synthesis of AMCs of ceramic particles with the aluminium matrix is wettability in the casting route, and it was overcome by adding 2% of magnesium in the melt, proper incorporation time, and appropriate stirring speed. The microstructure and mechanical characteristics of the synthesized AMC were analyzed. Si_3N_4 particles in the matrix are uniformly dispersed in the optical and scanning electron micrographs (SEM). Adding reinforcement particles of Si_3N_4 to the AA6061 matrix increased microhardness, macrohardness, and ultimate tensile strength significantly. Microhardness and macrohardness of the AA6161/20 wt.% Si_3N_4 composite were 98 VHN and 91 BHN, respectively, which were 117.8% and 111.63% higher than those of the AA6061 matrix alloy, respectively. Ultimate tensile strength (UTS) of AA6061 was 159.82 MPa which was increased to 249.12 MPa in the AA6061/20 wt.% Si_3N_4 composite. Percent elongation of the $AA6061/Si_3N_4$ composite was reduced with the addition of Si_3N_4 reinforcement.

1. Introduction

Industry 4.0 demands novel materials, and the demand for monolithic alloys is decreasing as they could not meet the requirements of the modern structural applications. Advanced materials such as aluminium metal matrix composites (AMCs) are a new generation of materials and find a wider scope in aeronautical, automobile, and electronics parts' and turbine blades' applications owing to their attractive mechanical and structural properties of lightweight and high strength, better wear and fatigue resistance, greater stiffness, and highly effective electrical and thermal conductivities [1, 2]. They also exhibit high stability at elevated temperatures. Even though many processes such as squeeze casting technique, powder metallurgy, in situ reaction, and powder injection moulding are employed to synthesize AMCs, stir casting route is commonly employed commercially as it has many advantages over other processing methods.

Stir casting is one form of casting process where a mechanical stirrer is used to mix the reinforcement with the

matrix base material such as aluminium by forming a vortex. Stir casting is one of the most effective methods for mass fabrication of AMCs because it is simple, flexible, economical, and suitable for mass production and production of complex profiled composite components without damaging the reinforcement particles [3, 4]. A typical stir casting machine comprises a mechanical feeder, reinforcement stirrer, and furnace that withstands high temperature and is used for melting of aluminium matrix materials.

The stir casting process involves various steps such as the following: (a) melting of the matrix aluminium materials; (b) stirring of molten matrix materials by using a mechanical stirrer; (c) feeding of reinforcement materials that have higher melting point than matrix materials. Generally, reinforcements are preheated before using in the matrix solution; (d) continuous stirring of the mixture of reinforcement and matrix; (e) pouring of the mixture in the mould after ensuring proper distribution of reinforcement throughout the matrix; (f) solidification of the mixture for further processing and testing. Mechanical properties of the AMCs depend on the effective distribution of the reinforcements in the matrix which in turn depends on the proper stirring of the mixture. These dispersions depend on the stirring parameters such as stirring speed, stirring time, position of the stirrer, stirrer size, and the feed rate of the reinforcements [5].

Kalaiselvan et al. [6] fabricated the AMC reinforced with various (viz., 4, 6, 8, 10, and 12) wt.% of B_4C by using the stir casting process and studied its metallurgical and mechanical properties. The K_2TiF_6 flux added to improve the wettability was reacted with B_4C particles and produced K and F compounds which contributed for removing the oxide film from the Al surface. Macrohardness, microhardness, and UTS of the AMC reinforced with 12% of B_4C were 58%, 70%, and 16% higher than those of 4% of B_4C particles, respectively. Wahab et al. [7] fabricated the Al-Si alloy reinforced with the AlN composite by the stir casting process. No porosity was observed in the microstructure which might be due to optimum stirring speed of the slurry and good bonding. Pazhouhanfar and Eghbali [8] fabricated the AA2024 matrix composite reinforced with Al_2O_3 particles of various sizes viz., 16, 32, and 66 μm by the stir casting route. The dispersion of the coarser size (66 μm) was more uniform, while the finer particles (16 and 32 μm) were led to agglomeration and segregation of the particles and porosity. It was justified that the Al dendrites solidified first during solidification of the composite, and the particles were rejected by the solid-liquid interface and, hence, were segregated to the interdendritic region. This event occurred more easily with the finer particles. Both hardness and tensile strength increased with the amount of Al_2O_3 particles present and decreasing particle size.

Several studies have shown an incremental value in the mechanical properties such as hardness and tensile properties with an increase in reinforcement weight percentage in AMCs [9–11]. Also, studies on AA6082/Si_3N_4 are found to increase in wear resistance and hardness properties [12, 13]. In this study, silicon nitride (Si_3N_4) was reinforced in AA6061 alloy, and its mechanical and metallurgical characterizations were analyzed.

2. Experimental Procedure

Wolfram-coated stainless steel crucibles of the electric furnace were used to heat a predetermined quantity of heat-treatable aluminium alloy AA6061-T6 (Mg-0.9, Si-0.64, Fe-0.26, Cu-0.21, Mn-0.1, Cr-0.05, Zn-0.04, Ni-0.02, Ti-0.01, and Al-balance by wt.%) rods which are shown in Figure 1. Wolfram coating prevents the contamination of melt at higher temperature. Crucible temperature was set to 1000°C. When the crucible attained 600°C, it was supplied with a constant volumetric flow of argon gas of 2 liters per min which is applied to prevent the aluminium alloy from reacting chemically with oxygen and nitrogen in the atmosphere. When the crucible attained 1000°C, the wettability of the alloy was enhanced by adding magnesium (2%) with the metal between Si_3N_4 and AA6061 alloy. The melt was stirred at 400 rpm using a Wolfram-coated stainless steel stirrer and an electric motor. It is imperative that stirring of the molten alloy aids the incorporation of the reinforcement particles Si_3N_4 in the AA6061 alloy and facilitates homogeneous dispersion. Appropriate stirring speed must be maintained to avoid entrapment of the gas in the molten alloy which may form because of overagitation of the melt and lead to poor quality of the cast. A predetermined amount (15% of weight of the composite to be produced) of Si_3N_4 particles of size 5 to 6 μm and purity of more than 99.6% was preheated to 750°C in a separate electric furnace which is shown in Figure 2. Preheating of Si_3N_4 was done (i) to remove all the moisture and trapped air between the reinforcement particles, (ii) to reduce the temperature gradient between the molten alloy and reinforcement particle which would increase the viscosity of the slurry as the result of difficulties in eliminating the trapped gases, and (iii) to remove the impurities from the surface of the particles. Preheated Si_3N_4 was added into the molten matrix, and the slurry was stirred for 1200 s. Without stopping the stirring and supply of the argon gas, the slurry was poured through the bottom pouring attachment into the cavity of the preheated permanent die at 300° C. Figure 2 shows the permanent die and electric preheater. The composites were solidified in the ambient condition. Similarly, AA6061 matrix containing 20 wt.% of Si_3N_4 and AA6061 alloy were fabricated. The fabricated AA6061 alloy and AA6061/15 and 20 wt.% Si_3N_4 composite castings are presented in Figure 3.

To perform the metallurgical characterization, specimens of size 25 mm × 25 mm × 6 mm were taken out from the cast alloy and composite containing 15 and 20 wt.% of Si_3N_4. As per the standard metallographic techniques, all the specimens were prepared. The specimens have been polished with emery sheets from 280 to 1200 grit and further polished using a disc polishing machine by diamond pastes of sizes 6, 3, and 0.5 m. Acetone and purified water were used to clean the polished specimens completely. The cleaned specimens were etched for microstructural analysis by means of a colour etchant solution of 1 g of sodium hydroxide (NaOH) and 4 g of potassium permanganate ($KMnO_4$) in 100 ml of distilled water. Optical microscope (Olympus BX51M) and scanning electron microscope (SEM) were used to observe the microstructural analysis of the etched specimens. Brinell

Figure 1: Modified electric stir casting furnace with the bottom pouring attachment and the electric furnace used to preheat Si_3N_4.

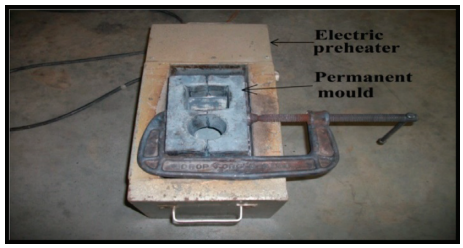

Figure 2: Preheater of the permanent mould.

hardness tester (model 7KB3000) with an axial load of 500 kg operated for 15 seconds at ten separate sites was used to determine the macrohardness of the AA6061 alloy and AA6061/15 and 20 wt.% Si_3N_4. With a microhardness tester (Mitutoyo MVK-H1), the specimens were tested by placing a 500 g load for 15 seconds on 25 different spots. From each cast composite and AA60601 alloy, 2 tensile specimens were cut as per the American Society of Testing and Materials (ASTM: E8/E8 M-11) standard [14]. The tensile specimen dimensions according to the ASTM standard are presented in Figure 4. The fabricated tensile specimens as per the ASTM standard are shown in Figure 5. A computerized universal testing machine (HI-TECH TUE-C-1000) was used for determining the ultimate tensile strength (UTS) and percent elongation (PE) at ambient temperature, and the standard values were recorded.

3. Results and Discussion

The matrices of the AA6061 alloy reinforced with 15 and 20 wt.% of Si_3N_4 composites were successfully manufactured through the stir casting route with optimized process parameters. The metallurgical and mechanical characterization studies of the AA6061/Si_3N_4 fabricated composites are discussed below.

3.1. Microstructure of AA6061/Si_3N_4 Composites. The optical microstructures of the AA6061 alloy and AA6061 alloy-fabricated matrix composites reinforced with 15 and 20 wt.% of Si_3N_4 are shown in Figure 6. The optical microstructure of the cast AA6061 alloy can be observed in Figure 6(a). Alpha-aluminium dendritic network structures were found in the microstructure. Formation of the alpha-aluminium dendritic network structure is attributed to the rapid cooling of the AA6061 alloy during solidification. In the microstructure, precipitation of the inorganic compound magnesium silicate (Mg_2Si) is observed. Figure 6(b) reveals the micrographs of AA6061/15 and 20 wt.% Si_3N_4 composites, respectively. There are no signs of porosity or other casting defects in these micrographs, and the Si_3N_4 reinforcement particles are more uniformly dispersed in the aluminium alloy matrix. These indicate that proper casting procedure was employed to cast composites. The causes for refinement of alpha-aluminium grains are as follows: (i) during the solidification of the AA6061/Si_3N_4 composite, Si_3N_4 particles are pushed in the direction of refined alpha-aluminium grains and (ii) alpha-aluminium grains settle on Si_3N_4 particles, which act as a nucleus [15].

Figure 6(a) depicts the precipitation of Mg_2Si in the matrix. Magnesium silicide is formed from a variety of sources: (i) Si and Mg are the major constituents in the AA6061 alloy and (ii) the incorporation of magnesium into a molten alloy (for increasing the wettability between the AA6061 alloy and Si_3N_4 particles). Oxide layer inclusions and intermetallic compounds were not seen in the microstructure of composites. It may be due to the continuous supply of inert argon gas into the crucible. Figure 7 shows the SEM image of AA6061/15 and 20 wt.% Si_3N_4 composites. It is obvious from the SEM micrographs that dispersion of Si_3N_4 reinforcement particles in the matrix alloy is more homogeneous.

3.2. Assessment of Mechanical Properties. The microhardness values of the AA6061 alloy and AA6061/15 and 20 wt.% Si_3N_4 composites are shown in Figure 8. Both hardness of the composites increases linearly with the increase of hard Si_3N_4 reinforcement particles in the AA6061 alloy matrix. Microhardness of AA6061/15 and 20 wt.% Si_3N_4 composites is 86 VHN and 98 VHN, respectively, and these are 91.11% and 117.78% higher than those of the AA6061 matrix alloy, respectively. Microhardness of the AA661 alloy is 45 VHN. Similarly, macrohardness of AA6061/15 and 20 wt.% Si_3N_4 composites is 79 BHN and 91 BHN, respectively, and these are 83.72% and 111.63% greater than those of the AA6061 matrix alloy, respectively. Macrohardness of the AA6061 alloy is 43 BHN. Average UTS and elongation percentage of the AA6061 matrix and AA6061 matrix composites containing 15 and 20 wt.% of Si_3N_4 reinforcement particles are shown in Figure 9. UTS of AA6061/15 and 20 wt.% of Si_3N_4 was 229.48 and 249.12 MPa, respectively. The addition of Si_3N_4 particles (which are having a lower coefficient of thermal expansion of 3.7×10^{-6}/K) in the aluminium alloy (which is having a higher coefficient of thermal expansion of 24×10^{-6}/K) alters the microstructural changes in the matrix which enhances the strength of the composites. When the amount of Si_3N_4 ceramic particles in an aluminium matrix alloy is increased, the grain size and substructure of the matrix are reduced, while the dislocation density surrounding the Si_3N_4 particles increases during solidification [16].

Figure 3: Fabricated AA6061/Si_3N_4 composite castings.

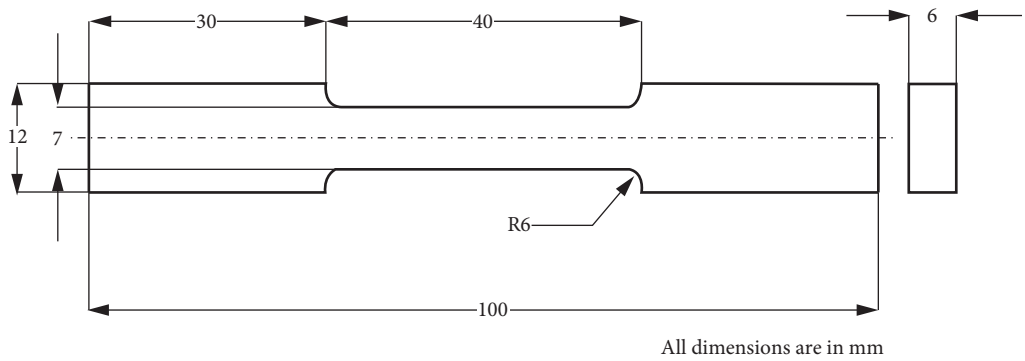

Figure 4: Dimensions of the tensile specimen as per the ASTM: E8/E8 M-11 standard.

During solidification, hard ceramic Si_3N_4 particles in the molten aluminium alloy provide additional heterogeneous nucleating sites. As a result, further decrease in grain size of the AA6061 matrix alloy is observed. All these microstructural changes increase the resisting force against the macroscopic- and microscopic-level dislocations under the action of a far-field stress [17]. As a result, an increase of Si_3N_4 in the matrix increases the hardness and UTS of the composites. The effect of reinforcement of Si_3N_4 on percent elongation (PE) of the composite is presented in Figure 9(b). The ductility of the aluminium matrix is reduced due to the following: (i) an increasing amount of hard Si_3N_4 in the AA6061 matrix which reduced the plastic flow of the matrix, (ii) more grain boundaries per unit area due to the grain refinement as the incorporation of reinforcement particles increases the number of turns of the dislocation path, and (iii) increased weight percentage of Si_3N_4 reinforcement particles in the composite reduces the volume fraction of the ductile aluminium alloy matrix. As a result of all these effects, PE of the composite is decreased with the addition of Si_3N_4-reinforced particles.

3.3. Fracture Morphology. AA6061 alloy and AA6061/20 wt. percent Si_3N_4 composite fracture surface is shown in Figure 10. The fracture surface of the AA6061 alloy is shown in Figure 10(a). The figure clearly indicates that aluminium alloys undergo a plastic flow during tensile loading. Many dimples are also visible. All these marks indicate that fracture occurred in the ductile mode. Figure 10(b) shows the fracture surface of the AA6061 composite containing 20 wt.% of Si_3N_4 particles. Size of the dimples in the fracture surface of the composite is less than that of the aluminium alloy. Degree of flatness of the surface is also increased in the fracture surface of the composite. It is apparent that ductility is reduced in the composite, and the failure mode of the

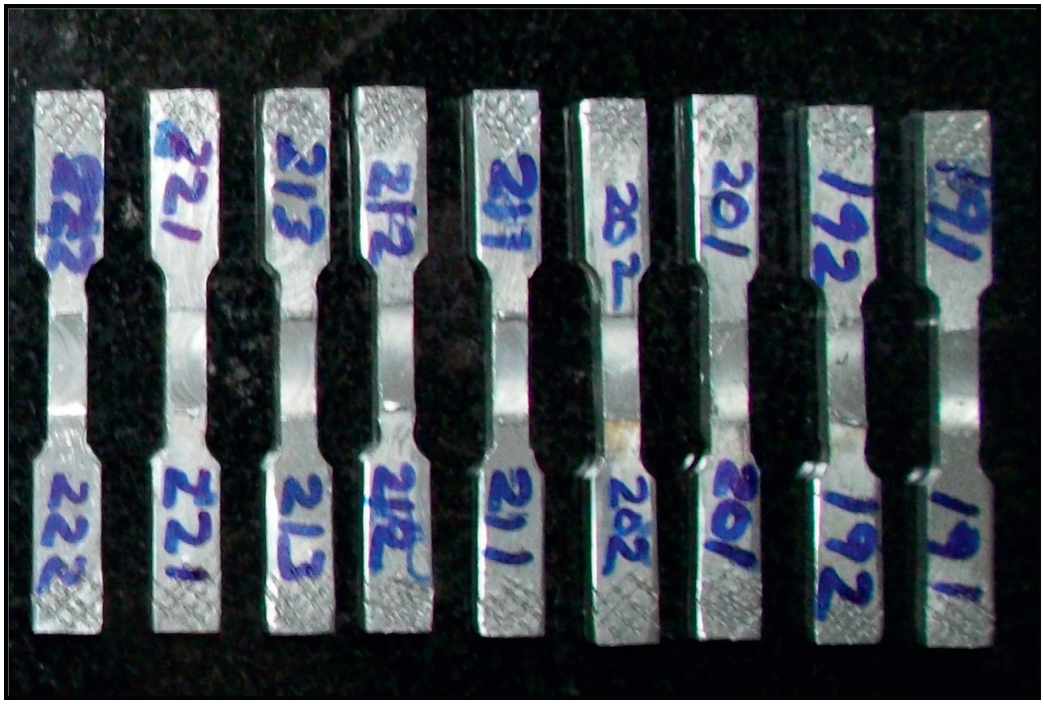

Figure 5: Fabricated tensile specimens as per the ASTM: E8/E8 M-11 standard.

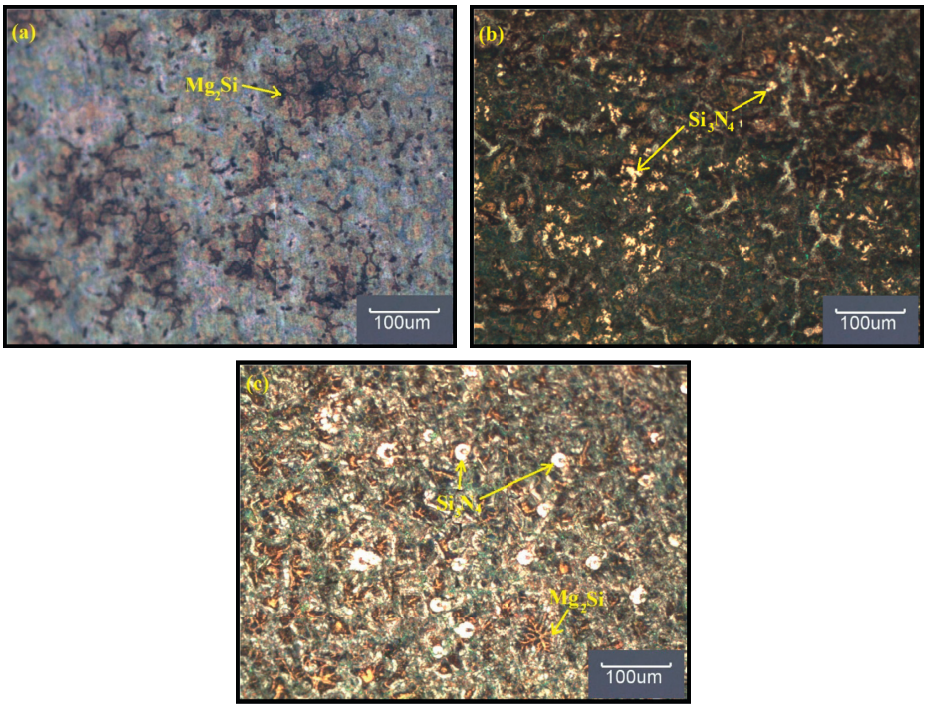

Figure 6: Optical photomicrograph of the (a) as-cast AA6061 alloy, (b) AA6061/15 wt.% Si_3N_4 composite, and (c) AA6061/20 wt.% Si_3N_4 composite.

composite is brittle. As the addition of reinforcement particles reduced the grain size, dislocations during tensile loading have less space before they hit a grain boundary. As dislocation is restricted by the grain boundary, plastic deformation is decreased, and the fracture mode becomes brittle [18].

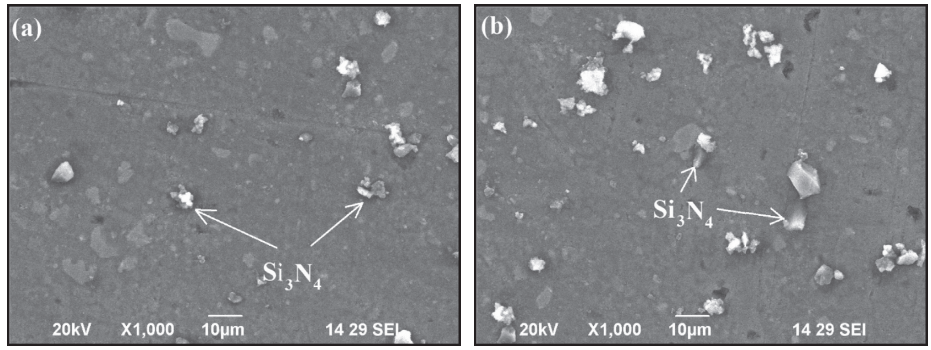

Figure 7: SEM micrograph of the (a) AA6061/15 wt.% Si_3N_4 composite and (b) AA6061/20 wt.% Si_3N_4 composite.

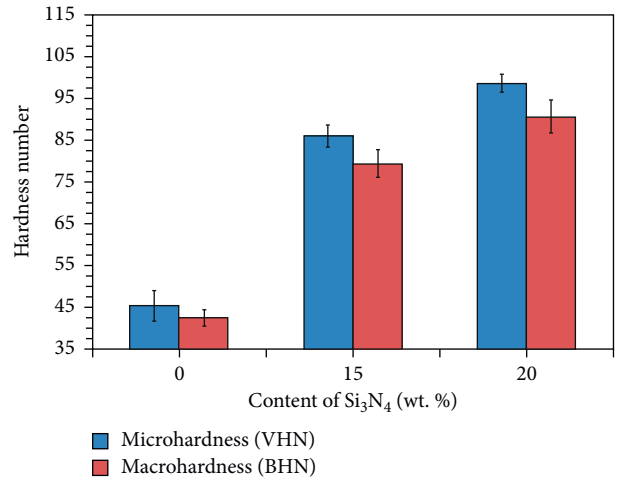

Figure 8: Effect of weight percentage of Si_3N_4 on microhardness and macrohardness of the Al/Si_3N_4 composite.

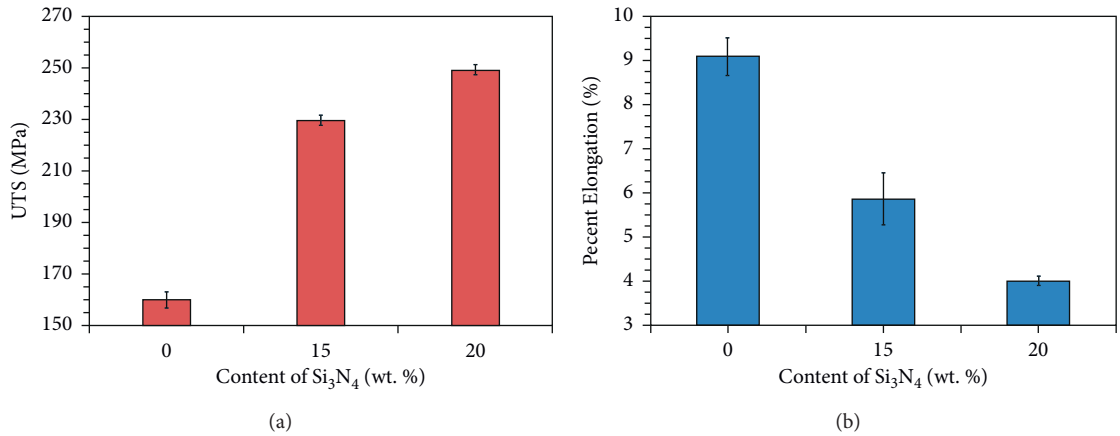

Figure 9: Effect of weight percentage of Si_3N_4 on (a) UTS and (b) PE of the AA6061/Si_3N_4 composite.

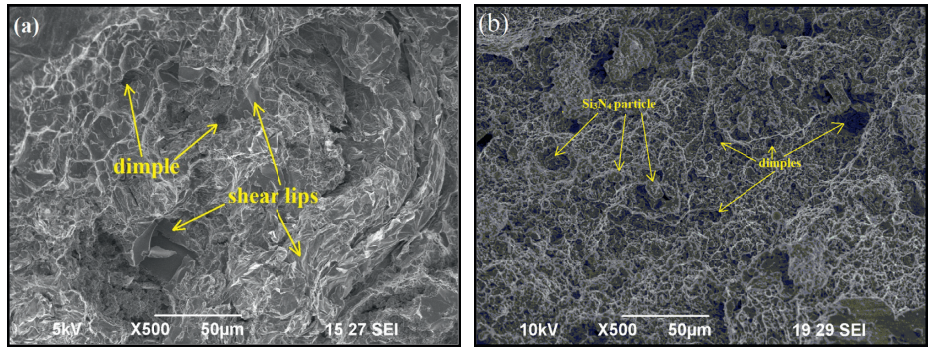

FIGURE 10: SEM micrographs of the fracture surface of the tensile specimen of (a) AA6061 alloy and (b) AA6061/20 wt.% Si_3N_4 composite.

4. Conclusions

(i) AA6061 alloy and AA6061 alloy matrix composite containing 15 and 20 weight percentage of Si_3N_4 reinforcement were successfully synthesized by the indigenously developed modified stir casting furnace with the bottom discharging attachment.

(ii) Si_3N_4 reinforcement particles were more uniformly dispersed in the AA6061 matrix.

(iii) Hardness and UTS of the AA6061/Si_3N_4 composite increased with the addition of Si_3N_4 particles. Microhardness and macrohardness of the AA6161/20 wt.% Si_3N_4 composite were 98 VHN and 91 BHN, respectively, which were 117.8% and 111.63% higher than those of the AA6061 matrix alloy, respectively. UTS of AA6061 was 159.82 MPa which was increased to 249.12 MPa in the AA6061/20 wt.% Si_3N_4 composite, but percent elongation of the composite reduced with the increase in the amount of particles. Percent elongation of the AA6061 alloy was 9 which was reduced to 4 in the AA6061/20 wt.% Si_3N_4 composite.

(iv) Failure mode of AA6061 and AA6061/20 wt.% Si_3N_4 composite was found to be ductile and brittle, respectively.

Data Availability

The data used to support the findings of this study are included within the article.

Conflicts of Interest

The authors declare that there are no conflicts of interest regarding the publication of this article.

Acknowledgments

The authors wish to place their sincere thanks to the Management and Department of Mechanical Engineering, Coimbatore Institute of Technology, Coimbatore, India, for extending the facilities of Welding Research Laboratory to carry out this investigation. They also wish to thank Karunya University, Coimbatore, India, for providing SEM and UTM testing facilities. They are also thankful to Mr. A. Raja for his assistance offered to execute the above work.

References

[1] J. Hemanth, "Quartz (SiO2p) reinforced chilled metal matrix composite (CMMC) for automotive applications," *Materials & Design*, vol. 30, no. 2, pp. 323–329, 2009.

[2] G. Naveen Kumar, R. Narayanasamy, S. Natarajan, S. P. Kumaresh Babu, K. Sivaprasad, and S. Sivasankaran, "Dry sliding wear behaviour of AA 6351-ZrB2 in situ composite at room temperature," *Materials & Design*, vol. 31, no. 3, pp. 1526–1532, 2010.

[3] S. Soltani, R. Azari Khosroshahi, R. Taherzadeh Mousavian, Z.-Y. Jiang, A. F. Boostani, and D. Brabazon, "Stir casting process for manufacture of Al–SiC composites," *Rare Metals*, vol. 36, pp. 581–590, 205.

[4] J. Jebeen Moses, I. Dinaharan, and S. Joseph Sekhar, "Prediction of influence of process parameters on tensile strength of AA6061/TiC aluminium matrix composites produced using stir casting," *Transactions of Nonferrous Metals Society of China*, vol. 26, no. 6, pp. 1948–1511, 2016.

[5] J. Hashim, L. Looney, and M. S. J. Hashmi, "Particle distribution in cast metal matrix composites-Part I," *Journal of Materials Processing Technology*, vol. 123, no. 2, pp. 251–257, 2002.

[6] K. Kalaiselvan, N. Murugan, and S. Parameswaran, "Production and characterization of AA6061-B4C stir cast composite," *Materials & Design*, vol. 32, no. 7, pp. 4004–4009, 2011.

[7] M. N. Wahab, A. R. Daud, and M. J. Ghazali, "Preparation and characterization of stir cast-aluminium nitride reinforced aluminium metal matrix composites," *International Journal of Mechanical and Materials Engineering*, vol. 4, no. 2, pp. 115–117, 2009.

[8] Y. Pazhouhanfar and B. Eghbali, "Microstructural characterization and mechanical properties of TiB_2 reinforced Al6061 matrix composites produced using stir casting process," *Materials Science and Engineering: A*, vol. 710, pp. 172–180, 2018.

[9] V. Bharath, M. Nagaral, V. Auradi, and S. A. Kori, "Preparation of 6061Al-Al 2 O 3 MMC's by stir casting and evaluation of mechanical and wear properties," *Procedia Materials Science*, vol. 6, pp. 1658–1667, 2014.

[10] V. Mohanavel, K. Rajan, and M. Ravichandran, "Synthesis, characterization and properties of stir cast AA6351-Aluminium Nitride (AlN) composites," *Journal of Materials Research*, vol. 31, no. 24, pp. 3824–3831, 2016.

[11] V. Mohanavel and M. Ravichandran, "Experimental investigation on mechanical properties of AA7075-AlN composites," *Materials Testing*, vol. 61, no. 6, pp. 554–558, 2019.

[12] K. Shirvanimoghaddam, H. Khayyam, and H. Abdizadeh, "Effect of B_4C, TiB_2 and $ZrSiO_4$ ceramic particles on mechanical properties of aluminium matrix composites Experimental investigation and predictive modelling," *Ceramics International*, vol. 42, no. 5, pp. 6206–6220, 2016.

[13] R. Kumar Arya and T. Amit, "Silicon nitride as a reinforcement for aluminium metal matrix composites to enhance microstructural, mechanical and tribological behavior," *International Journal of Engineering and Advanced Technology*, vol. 9, no. 3, pp. 3366–3374, 2020.

[14] ASTM Standard E8, *Standard Test Method for Tension Testing of Metallic Materials*, ASTM, International, West Conshohocken (USA), 2004.

[15] I. Dinaharan, N. Murugan, and S. Parameswaran, "Influence of in situ formed ZrB_2 particles on microstructure and mechanical properties of AA6061 metal matrix composites," *Materials Science and Engineering A*, vol. 528, pp. 5733–5740, 2011.

[16] B. Ashok Kumar and N. Murugan, "Metallurgical and mechanical characterization of stir cast AA6061-T6-AlN_p composite," *Materials and Design*, vol. 40, pp. 52–58, 2012.

[17] M. Gupta and TS. Srivatsan, "Interrelationship between matrix microhardness and ultimate tensile strength of discontinuous particulate-reinforced aluminium alloy composites," *Materials Letters*, vol. 51, pp. 255–261, 2001.

[18] B. Ashok Kumar, I. Dinaharan, and M. N. Microstructural, "Mechanical and wear properties of friction stir welded AA6061/AlN_p composite joints," *Journal of Materials Engineering and Performance*, vol. 31, no. 1, pp. 651–666, 2021.